HHS Public Access

Author manuscript

Nat Chem Biol. Author manuscript; available in PMC 2010 April 01.

Published in final edited form as:

Nat Chem Biol. 2009 October ; 5(10): 765–771. doi:10.1038/nchembio.215.

Genetic mapping of targets mediating differential chemical phenotypes in *Plasmodium falciparum*

Jing Yuan[1], **Ronald L. Johnson**[2], **Ruili Huang**[2], **Jennifer Wichterman**[2], **Hongying Jiang**[1], **Karen Hayton**[1], **David A. Fidock**[3], **Thomas E. Wellems**[1], **James Inglese**[2], **Christopher P. Austin**[2], and **Xin-zhuan Su**[1]

[1]Laboratory of Malaria and Vector Research, National Institute of Allergy and Infectious Diseases, Bethesda MD 20892, USA

[2]NIH Chemical Genomics Center, National Human Genome Research Institute, National Institutes of Health, Bethesda MD 20892, USA

[3]Department of Microbiology, Columbia University, New York, NY 10032, USA

Malaria is a serious public health burden that causes an estimated 1–2 millions deaths and 300–500 million infections each year1. There is no effective vaccine available, and parasites resistant to almost all antimalarial drugs currently in use have been reported, including reduced sensitivity to derivatives of the traditional Chinese medicine qinghaosu (artemisinin, **2**)2. Development of new drugs and a better understanding of the targets of antimalarial drugs and drug resistance are urgently needed.

Phenotypic characterization of human malaria parasites is limited because pathogenic stages live within red blood cells (RBCs) and laboratory models for *in vivo* investigations are often unsatisfactory. Changes in response to antimalarial drugs, differences in growth rate, or variations in virulence are among the few phenotypes typically accessible3. When phenotypes are available, genetic mapping is a powerful tool to assign them to particular determinants, and various high-throughput genotyping methods, including microarrays for detecting single nucleotide polymorphism (SNPs) and microsatellites (MS), have been developed for studies of *Plasmodium falciparum* traits4. However, there are ~5,400 predicted genes in the parasite genome, and the function of the majority of these genes remains unknown5. Characterizing phenotypic differences in malaria parasites and identifying the genes affecting the differences may provide important information for investigating gene function.

Correspondence should be addressed to X.-Z.Su (xsu@niaid.nih.gov)..

AUTHOR CONTRIBUTIONS J.Y., drug assay qHTS, parasite culture, and data analysis; R.L.J., drug assay and qHTS, data analysis, and writing; J.W., qHTS; R.H., data analysis; H.J, drug assays; K.H., progeny cloning and writing; D.A.F., transfected parasites and writing, T.E.W., progeny and writing; C.P.A. and J.I., project planning and writing; X-z S., project conception, data analysis and writing.

Note: Supplementary information is available on the Nature Chemical Biology website.

COMPETING INTERESTS STATEMENT The authors declare that they do not have any competing financial interests.

A challenge in understanding drug action and mechanisms of drug resistance is to identify the relevant molecular target. One useful strategy is to synthesize an active compound and use it to affinity purify the protein target(s) to which the compound binds6. This approach, however, generally requires compounds that have high affinity for their targets. Another strategy employs genetic mapping to link chromosomal loci that affect parasite responses to compounds, allowing molecular targets to be identified after fine mapping and functional characterizations of candidate genes. In addition to discovering potential new antimalarial compounds, these strategies can detect and define differential chemical phenotypes (DCPs) that show distinct signature responses to compounds among a variety of parasite isolates.

Here we demonstrate a strategy for identifying targets of chemical compounds in malaria parasites by integrating quantitative high-throughput screening (qHTS) with genetic mapping (Fig. 1). We tested seven *P. falciparum* lines, including parents of three genetic crosses7–9, for their responses to 1,279 bioactive compounds and identified candidate genes for three DCPs using progeny from a genetic cross and genetic transfection methods of allelic replacement. These results show that differential responses of small molecules between parasite lines can be reliable phenotypes for exploring molecular mechanisms of pharmacologic interest. This study also provides an effective approach for investigating drug action and resistance mechanisms in diseases other than malaria.

RESULTS

Quantitative high-throughput screening of bioactive compounds using a *Plasmodium* proliferation assay

We tested *P. falciparum* proliferation within infected erythrocytes against the LOPAC^{1280} collection of known bioactives (Sigma-Aldrich) by a qHTS 10 of a SYBR DNA binding assay11. Parasite proliferation was measured after 72 hr of incubation (corresponding to 1.5 generations of intra-erythrocytic parasite growth), with each compound tested at seven or eight five-fold dilutions beginning at 29 μM. Two independent screens of each parasite line performed well, showing 0.7 or higher average Z' factor and eight-fold or higher signal-to-background ratio (Supplementary Table 1). The potencies of known antimalarial agents had similar values determined by the assay in 96-well plate format. Titrations of two control inhibitors, **2** and mefloquine (**3**), were present on every plate and showed expected IC_{50} values (Supplementary Table 1). The antimalarial agents chloroquine (**4**) and quinine (**5**) were present in the collection, and IC_{50} values determined from the qHTS for **5** were similar, but the measurements for **4** were 15- to 20-fold higher than those from 96-well plate tests (Supplementary Table 1) because of lower solubility of **4** in dimethyl sulfoxide (DMSO) (data not shown). Although the determined potencies of **4** were lower, the relative potency between lines sensitive to **4**, HB3, 3D7, and D10 were clearly distinguished from resistant lines. The consensus IC_{50} and activity values for each of the 1,279 compounds in each of the seven *P. falciparum* lines are listed in Supplementary Table 2 and screening data are deposited in PubChem (AID1828). Comparison of the replicate runs for each parasite line indicated excellent agreement of curve class assignment and IC_{50} determination. About 80% of actives (compounds associated with Class 1.1, 1.2, and 2.1 curves10; see Methods for curve class definitions) identified in one replicate were active in the second replicate for

all lines except Dd2, where 55% were active in both replicates. Of the actives that did not repeat, almost all showed inconclusive activity (Class 2.2 and 3) in the other replicate with few or none scoring as inactive (Supplementary Table 3). The potencies of compounds scored as active or inconclusive in both replicates correlated well (Supplementary Fig. 1), indicating good repeatability in determining IC_{50} values between replicates.

Discovery of potential antimalarial compounds

Screens of the seven parasite lines revealed a large number of consensus actives (active in both replicates or active in one replicate and inconclusive in the other), all of which inhibited parasite growth. Among the 1,279 compounds tested, about 20% to 30% were active in most lines except W2, where 40% were active, and D10 and Dd2, where 19% and 15% were active, respectively (Supplementary Table 3). Of the hundreds of inhibitors identified for each line, about 50% or more showed IC_{50} values between 1 and 10 μM and 6% to 14% had IC_{50} values less than 1 μM (Supplementary Table 4). There were 155 compounds that inhibited growth in all seven lines tested (Supplementary Table 5). The potency distribution of these pan inhibitors indicated differences in sensitivity between the lines; W2 was most sensitive, with 32% of the compounds having IC_{50} values of 1 μM or less, while Dd2 was least sensitive with 7% below 1 μM. We identified 25 potent compounds that inhibited proliferation in all parasite lines at lower than 2 μM IC_{50} (Supplementary Table 6). Some of these compounds are well known antimalarial drugs (**5** and quinacrine [**6**]), while others such as hexahydro-sila-difenidol hydrochloride (**7**), dequalinium dichloride (**8**), taxol (**9**), and BW 284c51 (**10**) are not compounds used for malaria prophylaxis or treatment.

Identification of a large number of DCPs

One of our study objectives was to identify and profile differences in parasite responses to different chemicals. These differences can be considered phenotypes that derive from underlying variations in each parasite genotype. Hierarchical clustering of activity category (Fig. 2a) and IC_{50} values (Fig. 2b) of actives showed clear differences in the parasite responses to many compounds. We therefore compared compounds between each pair of parasite lines that showed a five-fold or greater difference in IC_{50} (see Methods for specific criteria). Applying these criteria, we identified 149 compounds (Supplementary Table 7) that produced 607 potential DCPs between the seven lines (Table 1). Interestingly, the three chloroquine-sensitive (CQS) parasite pairs had the smallest differences in response to the chemicals: seven DCPs for HB3 and 3D7, two for HB3 and D10, and seven for 3D7 and D10. There were 58 DCPs between the parents of the three genetic crosses, with seven between 3D7 and HB3, 23 between GB4 and 7G8, and 28 between Dd2 and HB3 (Table 1). These DCPs can be used to identify responsible loci or genes *via* linkage mapping of recombinant progeny from the crosses.

Mapping molecular targets underlying selected DCPs

To confirm that genes underlying DCPs could be identified using genetic mapping, we examined (**1**), trimethoprim (**11**), and triamterene [**12**]) because they exhibited relatively large differences in IC_{50} between the parents of a GB4×7G8 cross. **1** (Fig. 3a) is a

competitive serotonin receptor antagonist and has been used to treat migraine headache12,13. From the qHTS, **1** was ten times more potent in 7G8 (0.2 μM) compared with GB4 (2 μM). Follow-up tests in 96-well plates confirmed the IC_{50} difference between 7G8 (0.37 ± 0.01 μM) and GB4 (2.8 ± 0.37 μM; Fig. 3b). We then tested the **1** responses of 32 progeny from the cross and used the resulting IC_{50} values and genotypic data from 285 MS markers9 to map genetic loci controlling the difference in parasite responses (Fig. 3b). Quantitative trait loci (QTL) analysis identified a major locus on chromosome 5 with an LOD score of 16.4 and another locus on chromosome 12 having a LOD score of 3.0 (Fig. 3c). A perfect genotype-phenotype association was found within a ~150-kb segment of chromosome 5 bounded by crossovers at marker B7M114 in progeny JB8 and marker B5M86 in progeny XE7, LA10, and WE2 (Fig. 3b). This 150-kb segment contained *pfmdr1*, the gene encoding a homolog of the human P-glycoprotein (PfPgh-1) involved in drug resistance, and 33 other predicted genes (Supplementary Table 8). The smaller peak on chromosome 12 suggests that a second gene might modulate the response to **1** (Fig. 3c).

11 (Fig. 4a) is an antifolate that targets DHFR and is used mainly for prophylaxis and treatment of urinary tract infections14. In follow up assays, the parasite clone 7G8 had a much higher IC_{50} (37 ± 1.2 μM) to **11** than did GB4 (2.5 ± 0.2 μM). Analysis of responses of 32 GB4×7G8 progeny to **11** showed two groups of recombinants that were separated by a large difference in IC_{50} as well as some variation in IC_{50} within each group, particularly in the resistant group (Fig. 4b). QTL analysis identified a major peak on chromosome 4 with an LOD score of 15.6 and some minor peaks on chromosomes 6 and 11 with LOD scores lower than 1.5 (Fig. 4c). A perfect genotype/phenotype association was found at marker C4M69 within a segment of chromosome 4 bounded by crossovers at marker C4M19 in progeny DAN and at marker C3M35 in progeny AUD and JH6 (Fig. 4b). The chromosome 4 segment spanned ~59 kb DNA and contained ten genes (Supplementary Table 9), including the gene encoding *P. falciparum* dihydrofolate reductase (PfDHFR).

12 (Supplementary Fig. 2a) is a Na^+ channel blocker15 with activity against edema from heart, kidney, or liver disease. In assays with **12**, the 7G8 parasite had an IC_{50} at least 70 times higher than that of GB4 (Supplementary Fig. 2b). Thirty-two progeny from the 7G8 and GB4 cross were tested with **12**, and two groups were identified that were separated by large differences in IC_{50} with some variations in IC_{50} within each group (Supplementary Fig. 2b), suggesting contributions from one major and several minor genes. QTL analysis of the genotypes and phenotypes from the progeny mapped a major determinant to a locus on chromosome 4 with a LOD score of 14.1 and another locus on chromosome 12 with a LOD score of ~2.3. Like **11**, the response to **12** mapped to a ~59-kb locus defined by informative crossovers in the same three progeny between marker C4M19 (DAN) and marker C3M35 (AUD and JH6) (Supplementary Fig. 2b), containing *pfdhfr* and nine other genes (Supplementary Table 9). These results suggested that a single locus confers resistance to both **11** and **12**.

Mutations in PfPgh-1 confer resistances to DHMS

Among the genes in the chromosome 5 locus, *pfmdr1* was a primary candidate because it encodes an ABC transporter involved in drug resistance, and there are no known targets to **1**,

such as 5-HT serotonin receptor or α-adrenergic receptor, in the locus12,13,16. To investigate whether *pfmdr1* mediated differential susceptibility to **1**, we examined *pfmdr1* mutations and responses to **1** in parasite isolates from different regions of the world (Supplementary Table 10). There are five known nucleotide substitutions in the *pfmdr1* genes, resulting in codon polymorphisms for N86Y, Y184F, S1034C, N1042D, and D1246Y17,18. Examination of the *pfmdr1* haplotypes and **1** responses in the field isolates suggested that the N1042D substitution was associated with a greater than 50% reduction in IC_{50} and the S1034C substitution was associated with a further reduction of 50% or more (Supplementary Table 10). These mutations account for the majority of the difference between 7G8 (the New World *pfmdr1* haplotype) and GB4 (the Old World haplotype). The roles of N86Y, Y184F, and D1246Y changes on sensitivity to **1** were unclear, as parasites with the same substitutions had quite different IC_{50} values in some cases (Supplementary Table 10). Field isolates usually display substantial genetic heterogeneity and the differences in genetic background could contribute to the variations in IC_{50} values observed.

To evaluate the influence of genetic background on the IC_{50} measurements, we tested several parasite lines where the *pfmdr1* coding regions were replaced with versions carrying different polymorphisms by allelic exchange18,19. Parasites with substitutions on the background of D10, which has the same *pfmdr1* allele as GB4, and on the background of 7G8 have been reported 18. Five parasites with different *pfmdr1* alleles on 7G8 or D10 genetic backgrounds were compared (Supplementary Table 10). Measurements of IC_{50} values from three of the five parasites were consistent with the predicted drug-response phenotypes, whereas two parasites ($D10^{7G8/1}$ and $D10^{7G8/2}$) yielded discrepant results. We therefore designed PCR primers to amplify specific sequences from the two parasites (Supplementary Fig. 3). Sequencing of the PCR products showed that the *pfmdr1* alleles in the two parasites were not the reported sequences; instead, the amino acids deduced from the DNA sequences matched the IC_{50} values observed in our drug tests (NYCDY for $D10^{7G8/1}$ and NYSND for $D10^{7G8/2}$; Supplementary Table 10). The apparent discrepancies between genotype and phenotype may have arisen from the mislabeling of parasites or cross-contamination during *in vitro* culture.

Additionally, we tested six transfected lines with *pfmdr1* alleles exchanged in two progeny (GC03 and 3BA6) of a Dd2×HB3 cross19. **1** responses of these allelic-exchanged parasites showed that an amino acid change of N1042D reduced the **1** IC_{50} by more than half and changes of S1034C and D1246Y lowered it further to less than 300 nM (Supplementary Table 10). Although the F184Y change slightly reduced the IC_{50} in D10 and 3D7 parasites (compared with C2A and 224), the same change in $7G8^{D10}$ and $D10^{D10}$ had little effect, suggesting that the F184Y substitution had little influence on the response to **1**. Together, the results from field isolates and allelic exchanged parasite lines demonstrate a strong association of S1034C and N1042D substitutions and resistance to **1**. Of interest, verapamil, a compound that inhibits human P-glycoprotein and can reverse the effects of many antimalarial and anticancer drugs19, did not have any effect on parasite response to **1** (Supplementary Table 11).

Polymorphisms in PfDHFR confer resistance to 11 and 12

Variations in PfDHFR among the seven parasite lines support the association of differential parasite responses to **11** or **12**. Although the locus on chromosome 4 contained ten genes, we considered *pfdhfr* as the primary candidate for resistance to both **11** and **12**, because **11** is a known DHFR inhibitor14 and inhibition of human leukocyte DHFR activity by **12** has also been reported20. Many mutations in PfDHFR have been shown to contribute to parasite responses to antifolate drugs, particularly substitutions at amino acid positions at 51, 59, and 10821.Sequencing of the *pfdhfr* coding region showed only two codon changes between 7G8 and GB4, with GB4 encoding N51 and S108 and 7G8 encoding I51 and T108 (Supplementary Table 12). We also determined seven known polymorphic sites of PfDHFR at codons 16, 50, 51, 59, 82, 108, 140, and 164 from the five other parasites, but found alterations only at codons 51, 59, and 108 (Supplementary Table 12). Similar to the pattern of response to pyrimethamine, a DHFR antagonist, parasites with substitutions at three positions in the gene had higher IC_{50} values to either **11** or **12** than those with two substitutions, which in turn were more resistant to parasites having one substitution22. These results suggested that mutations in PfDHFR confer resistance to **11** and **12**.

To rule out the influence of genetic backgrounds on parasite response, we tested two 3D7 lines that were transformed to express integrated alleles of PfDHFR with S108T substitution from HB3 or triple N51I, C59R, and S108T substitutions from Dd2 (pDT-HB3 and pDT-Dd2; Supplementary Table 12)23. As expected for parasites with integrated alleles, DNA sequencing confirmed the PfDHFR genotypes in the two parasites, which revealed S/T mixed codons at position 108 for pDT-HB3, and mixed codons at positions 51, 59, and 108 for pDT-Dd2 (Supplementary Fig. 4 and Supplementary Table 12). The 3D7 parasite transfected with the HB3 PfDHFR allele had IC_{50} values similar to those of HB3, while the parasite transfected with Dd2 allele had even higher IC_{50} values, although the IC_{50} values were lower than that of Dd2 parasite. These results demonstrated that introduction of a mutant PfDHFR allele into a sensitive parasite increased the IC_{50} values to both drugs. Sequencing of DNA from progeny of the GB4×7G8 cross showed that *pfdhfr* alleles in these parasites also matched the phenotypes observed (data not shown). These results, obtained from parasite lines, transfected parasites, and progeny, demonstrate that polymorphisms in PfDHFR indeed confer differential responses to **11** and **12**.

DISCUSSION

Progeny from genetic crosses, high-density MS and SNP maps, and high-throughput genotyping methods4,24,25 provide a powerful platform to identify parasite genes involved in differential responses to bioactive compounds. As a proof of principle, we identified a large number of phenotypic variations (DCPs) between individual parasites and linked two genes to parasite responses to three compounds using genetic mapping. Identification of many DCPs is consistent with a highly polymorphic *P. falciparum* genome26–28. It may also be possible to map DCPs by genome-wide association studies using genetically heterogeneous parasite populations4. The DCPs identified here may lead to the identification of many target genes and to a better understanding of the molecular interactions within the parasite.

Several large-scale screens for antimalarial compounds have been described, most of which assayed compounds at one or two concentrations (typically 10 μM)11,29–33. In contrast, we measured parasite responses to each compound at concentrations across four orders of magnitude, allowing us to generate concentration-response curves and derive IC_{50} values for all tested compounds immediately (Supplementary Table 2). Many active compounds showed IC_{50} values less than 1 μM (Supplementary Table 6), some of which may be tested to treat malaria without extensive clinical trials because many of the compounds in the LOPAC collection have been used for treating human diseases. Our study also showed that a compound active against one parasite line was often not effective in killing other parasites with different genotypes.

The observation of more DCPs among parasites resistant to **4** suggests that mutations and compensatory changes selected by **4** may impact parasite responses to other chemicals. Similarly, Dd2 was derived from W2 after selection to **3**34, and Dd2 was more less sensitive to many compounds than W2 (Supplementary Table 3). These observations suggest that following drug selection, parasites may become more resistant to multiple antimalarial drugs more quickly, consistent with the proposal of parasites showing the accelerated resistance to multiple drugs (ARMD) phenotype35. Because Dd2 and W2 have a very similar genetic background but are known to differ in *pfmdr1* copy number, the variation in *pfmdr1*copy number may play a role in some differential responses.

Mutation and amplification of *pfmdr1* play a role in drug responses in *P. falciparum*18,36,37. There are some similarities in the associations of *pfmdr1* alleles to responses to **1** and antimalarial agents such as **2**, **3**, and halofantrine (**13**). Amino acid changes in PfPgh-1 (from NFCDY to NFSND) increase the IC_{50} values of **2**, **3**, and **13** by two to six fold and decrease the IC_{50} of **5** in some genetic backgrounds18,19. Likewise, **1** showed a higher IC_{50} in parasites containing the NFSND allele. However, the changes in IC_{50} to **2**, **3**, and **13** after allelic exchange might be parasite specific because 7G8 and GB4 have very similar IC_{50} values to both **2** and **3** (Supplementary Table 1). Because PfPgh-1 is an ABC transporter homolog, mutations in this protein may affect its ability to transport **1** and other drugs.

Although **12** is a known Na^+ channel blocker15, our results showing that **12** acts on PfDHFR were consistent with observations that **12** interferes with folate metabolism *in vitro* and *in vivo*20,38,39. Interestingly, the known chemical structures of DHFR inhibitors and epithelial sodium channel blockers share a similar amino-pyrimidine ring and tethered aryl group (Supplementary Fig. 5). It is possible that these structural features account for the inhibition of DHFR and some sodium channels and these proteins may share similar binding pockets40.

Our results showing that **1** interacts with or is transported by an ABC transporter instead of the expected 5-HT2B receptor highlights how such studies can identify “off-target” effects of bioactive molecules. The observation that mutations in an ABC transporter can alter sensitivity to **1** may provide important information for studies and treatment of migraine syndrome.

METHODS

Parasites and compounds

The *P. falciparum* lines used in this study have been described previously41, and their origins and responses to **2–5** are summarized in Supplementary Table 1. Parasites Dd2, HB3, GB4, 7G8, and 3D7 are parents of three separate genetic crosses7–9. Dd2 is a clone derived from W2 that was originally isolated from Southeast Asia34. Progeny of a genetic cross (GB4×7G8) were described recently9. Transgenic parasites with the gene encoding a homolog of the human P-glycoprotein (PfPgh-1) replaced by mutant alleles were reported previously18,19. The parasites described by Reed, *et al*.18 were obtained from MR4 (http://www.mr4.org). Parasites transfected with mutant genes encoding PfDHFR were described previously23. All parasites were cultured *in vitro* according to methods described42. Briefly, parasites were maintained in RPMI 1640 medium containing 5% human O^+ erythrocytes (5% hematocrit), 0.5% Albumax (GIBCO), 24 mM sodium bicarbonate, and 10 μg/ml gentamycin at 37°C with 5% CO_2, 5% O_2, and 90% N_2.

The LOPAC^{1280} collection (http://www.sigmaaldrich.com/chemistry/drug-discovery/validation-libraries/lopac1280-navigator.html) was purchased from Sigma-Aldrich and the compounds prepared and plated as described10. **1–5**, **11**, and **12** were purchased from Sigma-Aldrich and had purities of 98% or better.

In vitro drug assays

The SYBR Green viability assay (Supplementary Table 13) was adapted from methods described previously11,32. Briefly, 3 μl culture medium was dispensed into 1536-well black clear-bottom plates (Aurora Biotechnologies) using a Multidrop Combi (Thermo Fisher Scientific Inc.); 23-nL compounds in DMSO were added by a pin tool (Kalypsys), and 5 μl of *P. falciparum*-infected RBCs (0.3% parasitemia, 2.5% hematocrit final concentration) were added. The plates were incubated at 37°C in a humidified incubator in 5% CO_2 for 72 h, and 2 μl lysis buffer (20 mM Tris-HCl, 10 mM EDTA, 0.16% saponin, 1.6% triton-X, 10X SYBR Green I supplied as 10,000X final concentration by Invitrogen) was added to each well. The plates were mixed for 25 sec with gentle shaking and incubated overnight at room temperature in the dark. The following morning, fluorescence intensity at 485(14) nm excitation and 535(25) nm emission wavelengths was measured on an EnVision (Perkin Elmer) plate reader. The LOPAC^{1280} collection (Sigma Aldrich) was screened against each line at eight (seven for Dd2) five-fold dilutions beginning at 29 μM. Antimalarial drugs, **2** and **3**, and DMSO were included as positive and negative controls for each plate, respectively.

Follow-up SYBR Green assays in 96-well plate format were performed as described43. Briefly, 150 μl synchronized parasites diluted to 1% parasitemia with 1% hematocrit were mixed with 50 μl medium containing compound. Compound stocks (10 mM) were dissolved in ethanol or DMSO and tested at 11 two-fold dilutions in triplicate. The beginning concentration of each compound was adjusted depending on IC_{50} values from the initial qHTS. The plates were incubated at 37°C under 5% CO_2, 5% O_2, and 90% N_2 for 72 h, incubated for another 30 min after addition of 50 μl lysis buffer, and read in a FLUOstar

OPTIMA reader (BMG Labtech). Data were analyzed using software at the NIAID Bioinformatic Resource website (https://niaid-biocluster.niaid.nih.gov/cgi-bin/bipod2/index.cgi).

Data analysis

Analysis of compound concentration-response data from the qHTS was performed as previously described10. Plate reads were first normalized relative to the control inhibitor (0.29 μM **2**) and vehicle (DMSO) wells present on each plate and then corrected by an algorithm using vehicle-only control plates at the beginning and end of the compound plate stack. Concentration-response data for each compound were curve-fitted and categorized into four major classes as described10 using custom software (http://ncgc.nih.gov/pub/openhts/curvefit/). Briefly, compounds in Class 1 produce a complete response curve containing two asymptotes, while compounds in Class 2 have incomplete response curves containing one asymptote. Compounds in Class 1 and 2 curves are further divided based on efficacy, with subclasses 1.1 and 2.1 having 80% or greater efficacy and subclasses 1.2 and 2.2 having less than 80% efficacy. Compounds with Class 3 curves show activity only at the highest concentration or are poorly fit Class 1 or 2 curves with r^2 less than 0.9. Compounds with Class 4 curves are inactive and either do not have a curve fit or the curve fit is below three standard deviations of the mean basal activity (about 30% efficacy).

Compound activities were categorized as Active (Class 1.1, 1.2, or 2.1), Inconclusive (Class 2.2 or 3) or Inactive (Class 4). Consensus activity between two replicates was scored as Active (Class 1.1, 1.2 or 2.1 in both replicates or Class 1.1, 1.2 or 2.1 in one replicate and Class 2.2 or 3 in the other), Inconclusive (Class 2.2 or 3 in both replicates), and Inactive (Class 4 in one or both replicates). For determining the potencies of consensus actives (Supplemental Tables 4–6), the IC_{50} values of both replicates were averaged. Differentially active compounds were defined as having five-fold or greater IC_{50} diferences between pairs of parasite lines with IC_{50} values determined as follows: If active in both replicates or active in one replicate and inconclusive in the other replicate, curve fits with *P* values 0.05 or less were used or averaged. If inconclusive with curve fit *P* values 0.05 or less for both replicates, IC_{50} values were averaged. If inactive in both replicates, the IC_{50} value was set to 29 μM, the highest tested concentration. If inconclusive with a curve fit *P* value greater than 0.05 or inactive in one replicate, the IC_{50} value was not used. Unsupervised hierarchical clustering of compound consensus activities and parasite lines was performed using Spotfire DecisionSite (TIBCO Software Inc.).

DNA sequencing, genotyping, and quantitative trait loci (QTL) analysis

To verify nucleotide substitutions in the genes encoding PfPgh-1 and PfDHFR, primers specific to the genes were commercially synthesized to amplify DNA sequences with known polymorphic sites (Supplementary Fig. 3). PCR products were sequenced directly without cloning into a plasmid vector as described44. MS genotypes for the parents and progeny of the genetic GB4×7G8 cross have been reported9,24. QTL analysis was carried out using the J/qtl program45.

Supplementary Material

Refer to Web version on PubMed Central for supplementary material.

ACKNOWLEDGMENTS

This work was supported by the Divisions of Intramural Research at the National Institute of Allergy and Infectious Diseases and by the National Human Genome Research Institute and the NIH Roadmap for Medical Research, all at the National Institutes of Health. We thank J. Sa, J. Mu, L. Jiang, D. Raj, and M.J. López Barragán for help in drug assays; P. Shinn and D. VanLeer for compound management; D. Leja for assistance in artworks, and NIAID intramural editor B.R. Marshall for assistance.

References

1. Snow RW, Guerra CA, Noor AM, Myint HY, Hay SI. The global distribution of clinical episodes of Plasmodium falciparum malaria. Nature. 2005; 434:214–7. [PubMed: 15759000]
2. Noedl H, et al. Evidence of artemisinin-resistant malaria in western Cambodia. N Engl J Med. 2008; 359:2619–20. [PubMed: 19064625]
3. Su, X.-z.; Wootton, JC. Genetic mapping in the human malaria parasite Plasmodium falciparum. Mol Microbiol. 2004; 53:1573–82. [PubMed: 15341640]
4. Su, X.-z.; Hayton, K.; Wellems, TE. Genetic linkage and association analyses for trait mapping in Plasmodium falciparum. Nat Rev Genet. 2007; 8:497–506. [PubMed: 17572690]
5. Gardner MJ, et al. Genome sequence of the human malaria parasite Plasmodium falciparum. Nature. 2002; 419:498–511. [PubMed: 12368864]
6. Knockaert M, et al. Intracellular targets of cyclin-dependent kinase inhibitors: identification by affinity chromatography using immobilised inhibitors. Chem Biol. 2000; 7:411–22. [PubMed: 10873834]
7. Walliker D, et al. Genetic analysis of the human malaria parasite Plasmodium falciparum. Science. 1987; 236:1661–6. [PubMed: 3299700]
8. Wellems TE, et al. Chloroquine resistance not linked to mdr-like genes in a Plasmodium falciparum cross. Nature. 1990; 345:253–5. [PubMed: 1970614]
9. Hayton K, et al. Erythrocyte binding protein PfRH5 polymorphisms determine species-specific pathways of Plasmodium falciparum invasion. Cell Host Microbe. 2008; 4:40–51. [PubMed: 18621009]
10. Inglese J, et al. Quantitative high-throughput screening: a titration-based approach that efficiently identifies biological activities in large chemical libraries. Proc Natl Acad Sci U S A. 2006; 103:11473–8. [PubMed: 16864780]
11. Plouffe D, et al. In silico activity profiling reveals the mechanism of action of antimalarials discovered in a high-throughput screen. Proc Natl Acad Sci U S A. 2008; 105:9059–64. [PubMed: 18579783]
12. Pollock LA. Further experience with dihydroergotamine methanesulfonate in the treatment of migraine; with a note on the use of cafergone. Ann West Med Surg. 1949; 3:388–90. [PubMed: 15407298]
13. Mehrotra S, et al. Current and prospective pharmacological targets in relation to antimigraine action. Naunyn Schmiedebergs Arch Pharmacol. 2008; 378:371–94. [PubMed: 18626630]
14. Gangjee A, Jain HD, Kurup S. Recent advances in classical and non-classical antifolates as antitumor and antiopportunistic infection agents: Part II. Anticancer Agents Med Chem. 2008; 8:205–31. [PubMed: 18288923]
15. Busch AE, et al. Blockade of epithelial Na+ channels by triamterenes - underlying mechanisms and molecular basis. Pflugers Arch. 1996; 432:760–6. [PubMed: 8772124]
16. Schaerlinger B, Hickel P, Etienne N, Guesnier L, Maroteaux L. Agonist actions of dihydroergotamine at 5-HT2B and 5-HT2C receptors and their possible relevance to antimigraine efficacy. Br J Pharmacol. 2003; 140:277–84. [PubMed: 12970106]

17. Foote SJ, et al. Several alleles of the multidrug-resistance gene are closely linked to chloroquine resistance in Plasmodium falciparum. Nature. 1990; 345:255–8. [PubMed: 2185424]
18. Reed MB, Saliba KJ, Caruana SR, Kirk K, Cowman AF. Pgh1 modulates sensitivity and resistance to multiple antimalarials in Plasmodium falciparum. Nature. 2000; 403:906–9. [PubMed: 10706290]
19. Sidhu AB, Valderramos SG, Fidock DA. pfmdr1 mutations contribute to quinine resistance and enhance mefloquine and artemisinin sensitivity in Plasmodium falciparum. Mol Microbiol. 2005; 57:913–26. [PubMed: 16091034]
20. Schalhorn A, Siegert W, Sauer HJ. Antifolate effect of triamterene on human leucocytes and on a human lymphoma cell line. Eur J Clin Pharmacol. 1981; 20:219–24. [PubMed: 7286039]
21. Hayton K, Su X.-z. Genetic and biochemical aspects of drug resistance in malaria parasites. Curr Drug Targets Infect Disord. 2004; 4:1–10. [PubMed: 15032630]
22. Kublin JG, et al. Molecular markers for failure of sulfadoxine-pyrimethamine and chlorproguanil-dapsone treatment of Plasmodium falciparum malaria. J Infect Dis. 2002; 185:380–8. [PubMed: 11807721]
23. Wu Y, Wellems TE. Transformation of Plasmodium falciparum malaria parasites by homologous integration of plasmids that confer resistance to pyrimethamine. Proc Natl Acad Sci U S A. 1996; 93:1130–4. [PubMed: 8577727]
24. Su, X.-z., et al. A genetic map and recombination parameters of the human malaria parasite Plasmodium falciparum. Science. 1999; 286:1351–3. [PubMed: 10558988]
25. Hayton K, Su X.-z. Drug resistance and genetic mapping in Plasmodium falciparum. Curr Genet. 2008
26. Mu J, et al. Genome-wide variation and identification of vaccine targets in the Plasmodium falciparum genome. Nat Genet. 2007; 39:126–30. [PubMed: 17159981]
27. Jeffares DC, et al. Genome variation and evolution of the malaria parasite Plasmodium falciparum. Nat Genet. 2007; 39:120–5. [PubMed: 17159978]
28. Volkman SK, et al. A genome-wide map of diversity in Plasmodium falciparum. Nat Genet. 2007; 39:113–9. [PubMed: 17159979]
29. Weisman JL, et al. Searching for new antimalarial therapeutics amongst known drugs. Chem Biol Drug Des. 2006; 67:409–16. [PubMed: 16882315]
30. Chong CR, Chen X, Shi L, Liu JO, Sullivan DJ Jr. A clinical drug library screen identifies astemizole as an antimalarial agent. Nat Chem Biol. 2006; 2:415–6. [PubMed: 16816845]
31. Baniecki ML, Wirth DF, Clardy J. High-throughput Plasmodium falciparum growth assay for malaria drug discovery. Antimicrob Agents Chemother. 2007; 51:716–23. [PubMed: 17116676]
32. Kato N, et al. Gene expression signatures and small-molecule compounds link a protein kinase to Plasmodium falciparum motility. Nat Chem Biol. 2008; 4:347–56. [PubMed: 18454143]
33. Arastu-Kapur S, et al. Identification of proteases that regulate erythrocyte rupture by the malaria parasite Plasmodium falciparum. Nat Chem Biol. 2008; 4:203–13. [PubMed: 18246061]
34. Wellems T, et al. Chromosome size variation occurs in cloned *Plasmodium falciparum* on in vitro cultivation. Review Brazilian Genetics. 1988; 11:813–825.
35. Rathod PK, McErlean T, Lee PC. Variations in frequencies of drug resistance in Plasmodium falciparum. Proc Natl Acad Sci U S A. 1997; 94:9389–93. [PubMed: 9256492]
36. Cowman AF, Karcz S. Drug resistance and the P-glycoprotein homologues of Plasmodium falciparum. Semin Cell Biol. 1993; 4:29–35. [PubMed: 8095826]
37. Price RN, et al. Mefloquine resistance in Plasmodium falciparum and increased pfmdr1 gene copy number. Lancet. 2004; 364:438–47. [PubMed: 15288742]
38. Zimmerman J, Selhub J, Rosenberg IH. Competitive inhibition of folic acid absorption in rat jejunum by triamterene. J Lab Clin Med. 1986; 108:272–6. [PubMed: 3760669]
39. Montalar M, et al. Kinetic modeling of triamterene intestinal absorption and its inhibition by folic acid and methotrexate. J Drug Target. 2003; 11:215–23. [PubMed: 14578108]
40. Yuvaniyama J, et al. Insights into antifolate resistance from malarial DHFR-TS structures. Nat Struct Biol. 2003; 10:357–65. [PubMed: 12704428]

41. Mu J, et al. Multiple transporters associated with malaria parasite responses to chloroquine and quinine. Mol Microbiol. 2003; 49:977–989. [PubMed: 12890022]
42. Trager W, Jensen JB. Human malaria parasites in continuous culture. Science. 1976; 193:673–5. [PubMed: 781840]
43. Liu S, Mu J, Jiang H, Su X.-z. Effects of Plasmodium falciparum mixed infections on in vitro antimalarial drug tests and genotyping. Am J Trop Med Hyg. 2008; 79:178–84. [PubMed: 18689621]
44. Mu J, et al. Chromosome-wide SNPs reveal an ancient origin for Plasmodium falciparum. Nature. 2002; 418:323–326. [PubMed: 12124624]
45. Broman KW, Wu H, Sen S, Churchill GA. R/qtl: QTL mapping in experimental crosses. Bioinformatics. 2003; 19:889–90. [PubMed: 12724300]

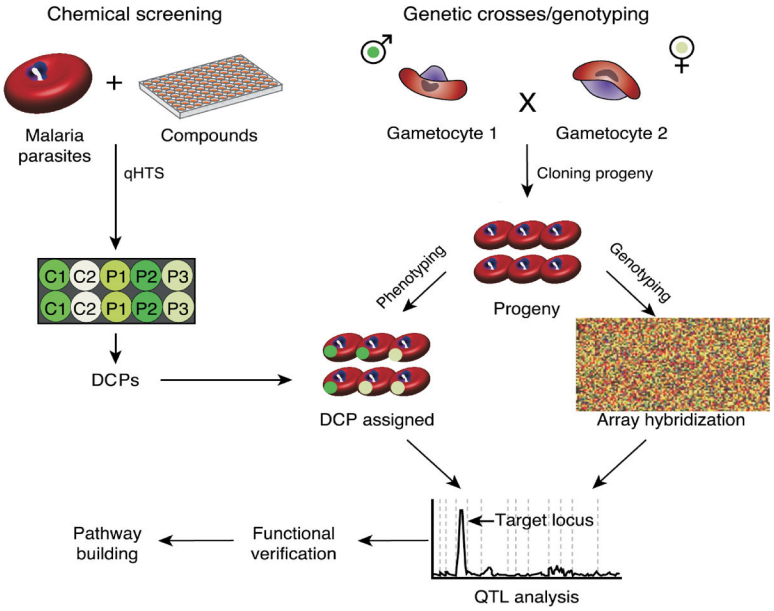

Figure 1.

A chemical genomic strategy for studying gene function in malaria parasites. Quantitative high-throughput screening (qHTS) of parasites against compounds in titration-response fashion identifies a large number of differential chemical phenotypes (DCPs). Target genes associated with these DCPs can be identified using quantitative trait loci analysis after genotyping progeny from genetic crosses or field isolates. Gene functions can be deduced from classes of compounds that target specific biologic pathways. The green circles represent differential parasite responses to chemicals. C1 and C2 represent negative and positive controls; and P1–P3 represent responses from three parasites. Gametocytes are the sexual stage of malaria parasite that can be cultured *in vitro*, and a genetic cross is started by feeding a mixture of gametocytes from two different parasites to mosquitoes.

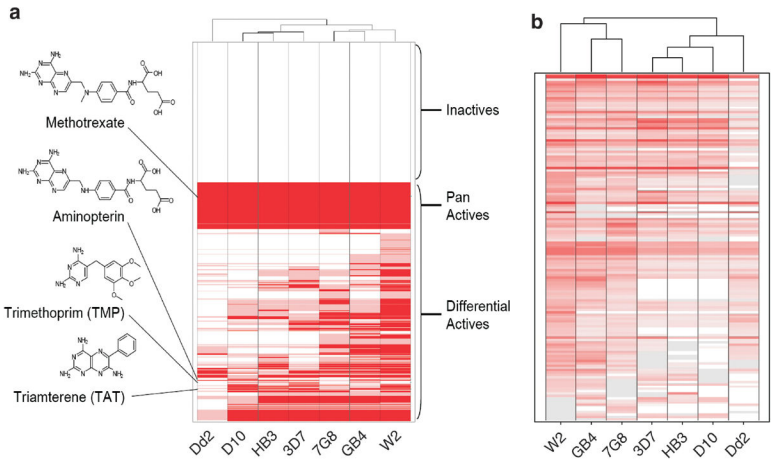

Figure 2.

Hierarchical clustering of compound activities in seven *Plasmodium falciparum* lines. (**a**) Clustering of compounds based on activity category from parasite responses to the compounds. Each compound was scored as consensus active (Class 1.1, 1.2, or 2.1 in one or both replicates; red), consensus inconclusive (Class 2.2 or 3 in both replicates; pink) or consensus not active (Class 4 in one or both replicates; white) for each parasite line. Structures of four known dihydrofolate reductase inhibitors and their positions in the clustering are shown. (**b**) Hierarchical clustering of IC_{50} values of differentially active compounds in seven *P. falciparum* lines. IC_{50} values of 149 compounds having five-fold or greater potency differences between two or more strains were clustered. IC_{50} values ranged from 12 nM (dark red) to > 29 μM (inactive; white). Grey indicates excluded IC_{50} values

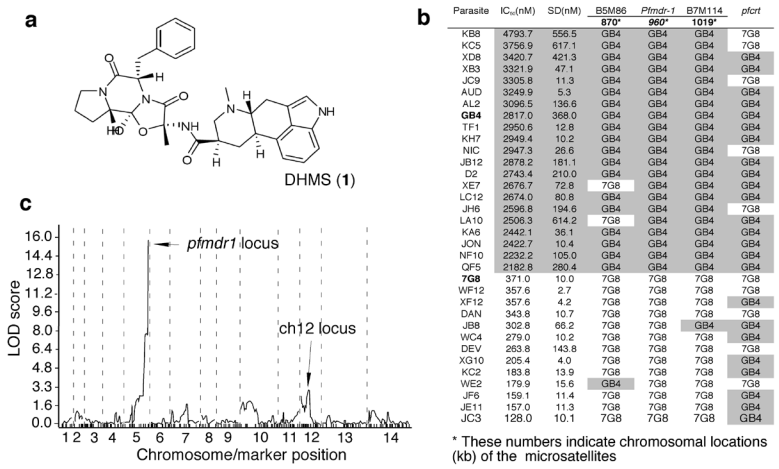

b

Parasite	IC_{50}(nM)	SD(nM)	B5M86 870*	*Pfmdr-1* 960*	B7M114 1019*	*pfcrt*
KB8	4793.7	556.5	GB4	GB4	GB4	7G8
KC5	3756.9	617.1	GB4	GB4	GB4	7G8
XD8	3420.7	421.3	GB4	GB4	GB4	GB4
XB3	3321.9	47.1	GB4	GB4	GB4	GB4
JC9	3305.8	11.3	GB4	GB4	GB4	7G8
AUD	3249.9	5.3	GB4	GB4	GB4	GB4
AL2	3096.5	136.6	GB4	GB4	GB4	GB4
GB4	2817.0	368.0	GB4	GB4	GB4	GB4
TF1	2950.6	12.8	GB4	GB4	GB4	GB4
KH7	2949.4	10.2	GB4	GB4	GB4	GB4
NIC	2947.3	26.6	GB4	GB4	GB4	7G8
JB12	2878.2	181.1	GB4	GB4	GB4	GB4
D2	2743.4	210.0	GB4	GB4	GB4	GB4
XE7	2676.7	72.8	7G8	GB4	GB4	GB4
LC12	2674.0	80.8	GB4	GB4	GB4	GB4
JH6	2596.8	194.6	GB4	GB4	GB4	7G8
LA10	2506.3	614.2	7G8	GB4	GB4	GB4
KA6	2442.1	36.1	GB4	GB4	GB4	GB4
JON	2422.7	10.4	GB4	GB4	GB4	GB4
NF10	2232.2	105.0	GB4	GB4	GB4	GB4
QF5	2182.8	280.4	GB4	GB4	GB4	GB4
7G8	371.0	10.0	7G8	7G8	7G8	7G8
WF12	357.6	2.7	7G8	7G8	7G8	7G8
XF12	357.6	4.2	7G8	7G8	7G8	GB4
DAN	343.8	10.7	7G8	7G8	7G8	7G8
JB8	302.8	66.2	7G8	7G8	GB4	GB4
WC4	279.0	10.2	7G8	7G8	7G8	GB4
DEV	263.8	143.8	7G8	7G8	7G8	7G8
XG10	205.4	4.0	7G8	7G8	7G8	GB4
KC2	183.8	13.9	7G8	7G8	7G8	GB4
WE2	179.9	15.6	GB4	7G8	7G8	7G8
JF6	159.1	11.4	7G8	7G8	7G8	GB4
JE11	157.0	11.3	7G8	7G8	7G8	GB4
JC3	128.0	10.1	7G8	7G8	7G8	GB4

* These numbers indicate chromosomal locations (kb) of the microsatellites

Figure 3.

Mapping genetic loci contributing to IC_{50} differences between 7G8 and GB4 in response to dihydroergotamine methanesulfonate (**1**). (**a**) Chemical structure of **1**. (**b**) IC_{50} values (mean and standard deviation) of **1** and allelic designations of three microsatellite markers on chromosome 5 and one at the gene encoding the chloroquine resistant transporter (*pfcrt*) on chromosome 7 are shown for the parents and progeny of a GB4×7G8 cross. A perfect match of sensitivity to **1** and microsatellite polymorphism in *pfmdr1* is seen. (**c**) Peaks of quantitative trait loci analysis linked to differential **1** responses are shown. Predicted genes within the chromosome 5 locus can be found in Supplementary Table 8.

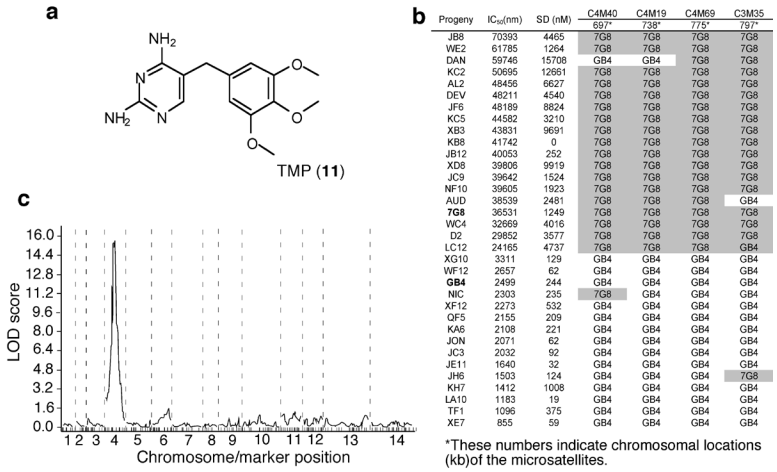

Figure 4.

Identification of genetic loci linked to response to trimethoprim (**11**). (**a**) Chemical structure of **11**. (**b**) IC_{50} values (mean and standard deviation) of **11** and allelic designations for three microsatellite markers on chromosome 4 are shown for the parents and progeny of a GB4×7G8 cross. (**c**) Peaks of quantitative trait loci analysis linked to differential responses to **11** are shown. Predicted genes within the chromosome 4 locus can be found in Supplementary Table 9.

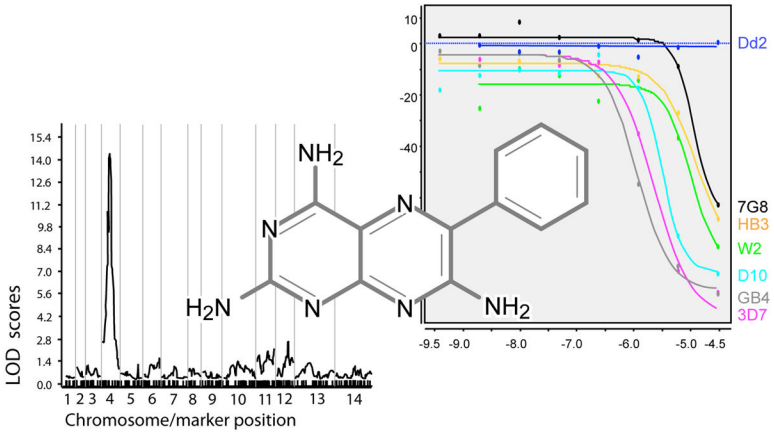

Figure 5.

Table 1

Number of potential differential chemical phenotypes from compounds with five-fold differences in IC_{50} values between parasite pairs

Parasite	3D7	7G8	D10	Dd2	GB4	HB3	W2
3D7	0						
7G8	23	0					
D10	7	34	0				
Dd2	33	21	31	0			
GB4	27	23	39	33	0		
HB3	7	18	2	28	26	0	
W2	39	21	74	53	16	52	0